View metadata, citation and similar papers at core.ac.uk
brought to you by CORE
provided by RERO DOC Digital Library

Tribol Lett (2012) 45:207–218
DOI 10.1007/s11249-011-9868-5

METHODS PAPER

In Situ Attenuated Total Reflection (ATR/FT-IR) Tribometry: A Powerful Tool for Investigating Tribochemistry at the Lubricant–Substrate Interface

Filippo Mangolini · Antonella Rossi · Nicholas D. Spencer

Received: 28 August 2011 / Accepted: 23 September 2011 / Published online: 11 October 2011
© Springer Science+Business Media, LLC 2011

Abstract To investigate the chemical changes occurring at metal/lubricant interfaces under tribological conditions in the boundary-lubrication regime, an in situ system for conducting quantitative tribological measurements has been constructed by combining an attenuated total reflection Fourier-transform infrared (ATR/FT-IR) spectrometer with a reciprocating tribometer. By periodically acquiring ATR/FT-IR spectra during sliding, spectroscopic changes due to thermal and/or tribochemical reactions occurring at the metal/oil interface can be monitored and correlated with friction measurements. The usefulness of this tribological test system has been demonstrated by performing ATR tribological experiments in the presence of a poly-α-olefin base oil at high temperature (423 K) on iron-coated germanium ATR crystals.

Keywords Attenuated total reflection Fourier-transform infrared (ATR/FT-IR) spectroscopy · In situ tribology · Uncertainty

F. Mangolini · A. Rossi · N. D. Spencer (✉)
Laboratory for Surface Science and Technology, Department of Materials, ETH Zurich, Wolfgang-Pauli-Strasse 10, 8093 Zurich, Switzerland
e-mail: nspencer@ethz.ch

Present Address:
F. Mangolini
Department of Mechanical Engineering and Applied Mechanics, University of Pennsylvania, 112 Towne Building, 200 S. 33rd Street, Philadelphia, PA 19104, USA

A. Rossi
Dipartimento di Chimica Inorganica ed Analitica, INSTM Unit, Università degli Studi di Cagliari, Cittadella Universitaria di Monserrato, 09100 Cagliari, Italy

1 Introduction

The development of surface-analytical methods over the recent decades has progressively allowed researchers in tribology to gain valuable insights into tribological—especially tribochemical—phenomena [1, 2]. The characterization of the films formed on solid surfaces under purely thermal conditions, or tribological conditions in the boundary-lubrication regime is fundamental for studying lubricant additives and understanding their mechanism of action [2]. Such experiments have mostly been performed ex situ, i.e., outside the tribometer and after the friction experiment [1]. After performing friction tests, the rubbed surfaces are usually cooled down, separated and removed from the test apparatus, washed with solvents (with the possible loss of weakly bound components), in many cases exposed to air, and then characterized in an environment that can be different from that found within the tribosystem. Although the ex situ approach provides the possibility of combining various complementary surface-analytical techniques, the analyzed surface might not be representative of the original material surface.

The recognition of these limitations, together with the need to study the kinetics of thermal film and tribofilm formation and the way in which they are influenced by different parameters (e.g., temperature, load, and sliding speed), has encouraged tribologists in the last decade to develop in situ techniques. In situ methods allow the direct probing of materials mechanics and chemistry characterizing the buried sliding interface as they form, in their "natural state" [1, 3]. The power of in situ studies in tribology has been recently highlighted in an issue of the *MRS Bulletin*, completely dedicated to the topic [3].

Among the analytical techniques used for carrying out in situ tribological investigations, molecular spectroscopies (i.e., infrared and Raman spectroscopy) were found to

provide a valuable insight into the chemical reactions taking place under steady-state conditions [4–22], but always require one of the rubbing surfaces to be transparent to the wavelength of radiation concerned.

Molecular spectroscopies have been the analytical techniques of choice for the development of *in contact* analytical approaches in tribology, which would allow the investigation of lubricant properties within the rubbing interface [14, 15]. Information about the chemical composition [23–25], the conformation of the lubricant film [15, 26] and the pressure distribution [27] can be gained by carrying out the analysis in the contact region.

Singer et al. developed an in situ Raman tribometer for investigating the third bodies formed in the contact by boric acid [7], Pb-Mo-S [6], diamond-like carbon (DLC) [5, 8–10], molybdenum disulphide [11, 12], and nanocomposite materials [4] and could determine how their morphology, structure, chemistry and motion impact the friction and wear behavior of solid lubricants. Using this in situ approach, the build-up, attachment, distribution and compositional changes of the third body could be followed during the tribological tests, used to identify variations in velocity-accommodation modes (VAM) and, therefore, correlated with frictional changes and instabilities. Even a quantification of the interfacial film thickness was possible on the basis of the intensity of the Raman signals.

ATR/FT-IR spectroscopy has been demonstrated to be a powerful tool for probing heterogeneous solid–liquid catalytic interfaces, since it provides information about the dissolved reactants and products in the bulk liquid and adsorbed intermediates as well as about the catalyst itself [28].

Previous work reported the development of an attenuated total reflection (ATR) FT-IR tribotester for the in situ characterization of boundary lubricant layers formed by anti-wear and extreme-pressure additives between iron-coated germanium ATR crystal and steel surfaces [17–19, 22]. The analytical capabilities of ATR/FT-IR spectroscopy were exploited for carrying out in situ tribological experiments: the iron/oil interface was investigated from "underneath", through a thin metallic iron layer representing one surface of the tribopair [17–19, 22]. By periodically acquiring ATR/FT-IR spectra, changes in the lubricant chemistry and the growth of reaction layers could be investigated as a function of different experimental parameters, such as temperature, normal load, and sliding speed.

The usefulness of this in situ ATR/FT-IR tribotester was demonstrated by investigating the thermal and tribochemical reactions of pure zinc dialkyldithiophosphate (ZnDTP)—the most widely used anti-wear additive since the 1940s—on iron surfaces at temperatures up to 423 K, as well as the effect of blending ZnDTP with a synthetic oil, i.e., poly-α-olefin (PAO), on the surface reactivity of this anti-wear extreme-pressure additive [17–19, 22]. ATR/FT-IR tribometry was also combined with X-ray photoelectron spectroscopy (XPS) and temperature-programmed reaction spectroscopy (TPRS) in order to study the surface chemistry of tributyl thiophosphate (TBT) on air-oxidized iron under purely thermal conditions and tribological conditions in the boundary-lubrication regime [20].

In this work, the ATR/FT-IR tribometer, developed in previous investigations [17–19, 22] for the in situ characterization of boundary lubricant layers formed by lubricant additives, has been extended and improved by the incorporation of a friction-force-measuring setup. This has allowed *quantitative* friction measurements to be obtained during tribological experiments and to be correlated, via spectroscopy, with the chemical changes taking place at the metal/oil interface.

2 In Situ Attenuated Total Reflection (ATR/FT-IR) Tribometer

2.1 Principle

An ATR/FT-IR spectrometer has been equipped with a new tribometer developed in collaboration with Ducom Instruments Pvt. Ltd. (Bangalore, India) on the basis of the previous version of the system designed and constructed in our laboratory in Zurich [17–19, 22].

The principle of the ATR/FT-IR tribometer is depicted in Fig. 1a. The tribological system consists of a fixed cylinder sliding in a reciprocating motion across the metal-coated ATR crystal surface. By periodically acquiring ATR/FT-IR spectra during tribological tests (the tribological test is stopped during the spectral acquisition and the counter-surface is lifted over the ATR crystal), the chemical changes taking place at the lubricant/metal interface due to thermal and/or tribochemical reactions can be investigated as a function of critical tribological parameters, such as applied load, sliding speed, temperature and sliding time, and correlated with friction measurements.

2.2 Design

The new version of the ATR/FT-IR tribometer comprises a testing block and a control block. The latter, which contains all the electronics and directly interfaces with the PC by means of a National Instrument PCI-6221 data acquisition (DAQ) board (installed in the PC), transfers the operating parameters to the tribometer and processes the signals coming from the load cell before transferring them to the PC. The testing block (Fig. 1b, c), mounted on top of the ATR unit, is fixed to the FT-IR spectrometer by means of four columns made of aluminum. A stepper motor (VEXTA Oriental Motor, model PK56W) is mounted on

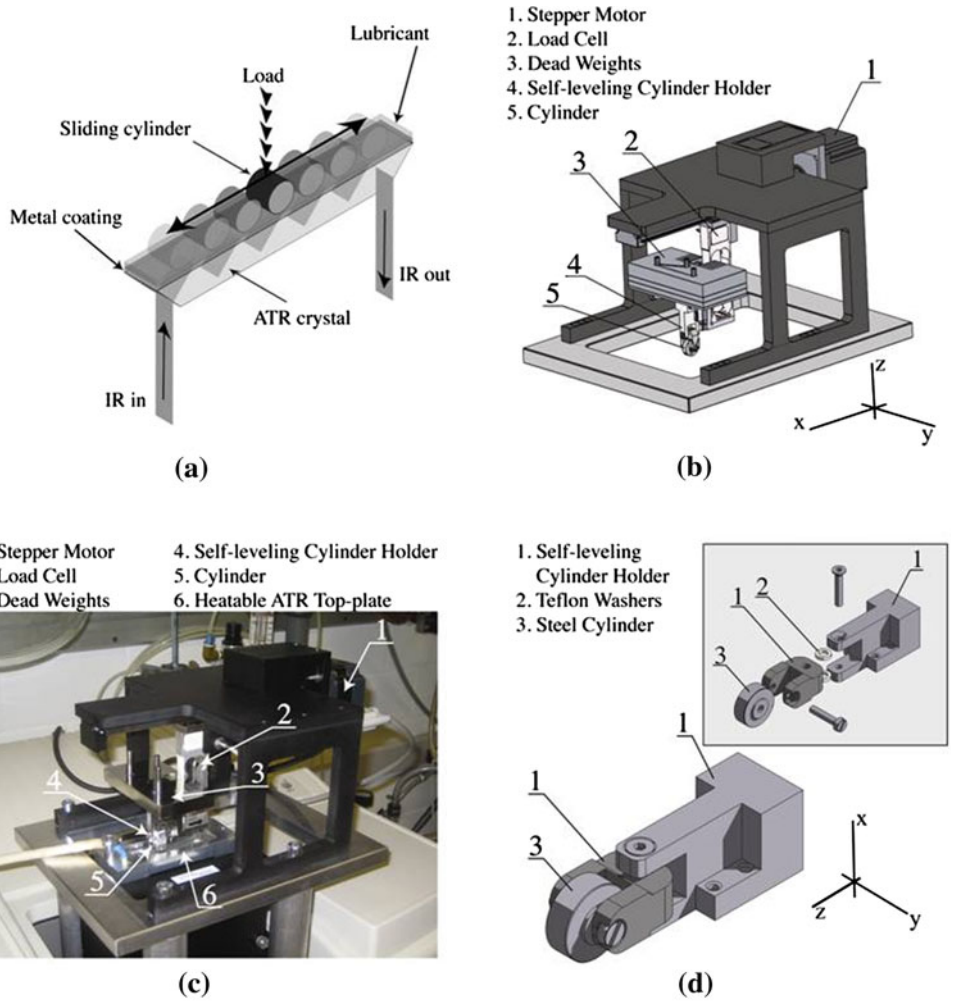

Fig. 1 Principle of ATR/FT-IR tribometry (**a**), 3D-CAD image (**b**), and picture (**c**) of the in situ ATR/FT-IR tribometer. A 3D-CAD drawing of the self-leveling cylinder holder used for ensuring a line contact between the cylinder and the ATR crystal is shown in **d**. The tribometer has been developed in collaboration with Ducom Instruments Pvt. Ltd. (Bangalore, India)

the tribometer and moves a one-dimensional load cell (Anyload model 108AA, Anyload Transducer Co. Ltd., Burnaby, B.C., Canada), used for registering the friction force, in a reciprocating motion across the counter-surface, i.e., the metal-coated ATR crystal, by means of a linear stage actuated by a worm drive.

The normal load is applied with dead weights fixed on top of the upper sample (cylinder) holder. The tribometer has a "frictionless" linear stage for dead weight loading.

The moving part of the tribopair, i.e., a fixed cylinder, is mounted on a self-leveling holder, fixed to the load cell, to ensure a line contact between the cylinder and the counter-surface (Fig. 1d).

The ATR crystal (angle of incidence of 45°, dimensions 72 × 10 × 6 mm (number of reflections, calculated according to [29], equal to 12) is mounted in a heatable (up to 473 K) top-plate for ATR units (Portmann Instruments AG, Biel-Benken, Switzerland) interfacing a temperature controller (FCS-23A, Shinko Technos CO., LTD, Japan). The temperature is measured with a PT-100 resistance element.

The tribological tests are programmed with Winducom 2006 (Ducom Instruments Pvt. Ltd., Bangalore, India), a software developed using LabVIEW (National Instruments Corporation), through which the test conditions (sliding speed, stroke, number of cycles, data save dwell) can be adjusted. During the experiment, normal load (F_Y, manually specified in the software), friction force (F_X), lateral position (*Stroke*) and cycle (C) are recorded.

Before each experiment, the planarity of the ATR crystal is checked using a spirit level, for coarse adjustments, and a dial indicator (Tesa Digico 1, Tesa Technology, Switzerland), for fine adjustments, fixed in place of the cylinder holder. By measuring the height of the ATR crystal at two points 50.0 ± 0.5 mm far away from each other and by placing aluminum foils between the tribometer and the columns through which the system is fixed to the FT-IR spectrometer, the planarity can be adjusted until it is better than ± 15 μm (over a 50.0 ± 0.5 mm distance), which corresponds to a maximum angular misalignment of 0.017°.

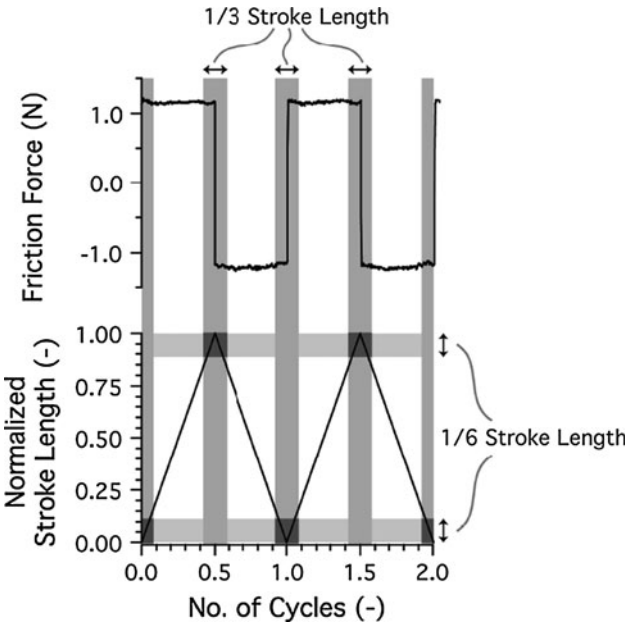

Fig. 2 Processing of the friction data: in order to avoid end-point effects, i.e., variation of the frictional data in correspondence of the positions where the sliding direction changes, only the data points corresponding to a cylinder position between 1/6 and 5/6 of the stroke length are considered for calculating the average coefficient of friction (CoF) and its standard deviation over one sliding cycle

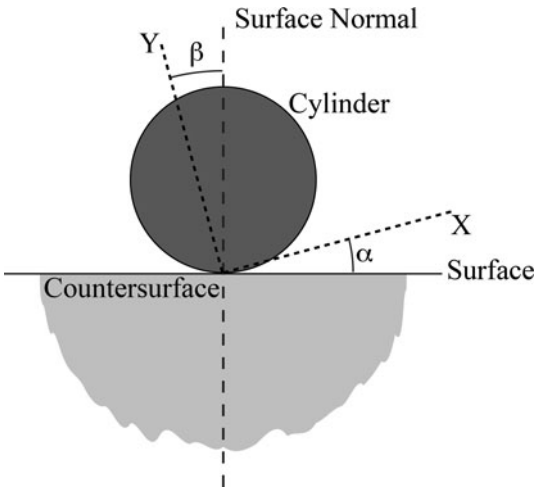

Fig. 3 Schematic of the force-measurement geometry. Due to errors in the adjustment of the sample planarity, the load cell axis intended to measure the normal force (axis Y) is misaligned by an angle β, whereas the load cell axis along which the friction force is intended to be measured (X) is misaligned by an angle α. In the general case, the measurement axes are not perpendicular (i.e., $\alpha \neq \beta$). Adapted from [32]

2.3 Data Processing

The friction coefficient is calculated as the ratio of the friction force (F_X) and the applied normal load (F_Y): $\mu = F_X/F_Y$. A time-averaging data-reduction method is applied for processing the frictional data by averaging the data acquired during one sliding cycle (one cycle equals two stroke lengths [30]). In order to avoid end-point effects, i.e., variation of the frictional data at the positions where the sliding direction changes, only the data points corresponding to a slider (or cylinder) position between 1/6 and 5/6 of the stroke length are considered (Fig. 2). The standard deviation of the values acquired during this period is also evaluated.

3 Uncertainty Analysis for the Attenuated Total Reflection (ATR/FT-IR) Tribometer

The uncertainty analysis reported here was performed following the methods described by Burris and Sawyer [31] and Schmitz et al. [32]. The uncertainties of the individual parameters (i.e., the friction force F_X, the normal load F_Y, the angular misalignment between the surface and the load cell axis along which the tangential force is measured α, the angular misalignment between the surface normal and the axis along which the normal force is applied β, see Fig. 3) have to be propagated into the calculations of the coefficient of friction according to the *Law of Propagation of Uncertainty* [33, 34]. The combined standard uncertainty for the friction coefficient ($u_c(\mu)$), which represents the minimum standard deviation of the friction coefficient results, has then to be calculated taking into account the standard uncertainty of each input parameter and the associated partial derivatives of the friction coefficient with respect to each input quantity (see Eq. 1). It has to be emphasized that this method assumes zero covariance between input values.

$$u_c^2(\mu) = \left(\frac{\partial \mu}{\partial F_X}\right)^2 u^2(F_X) + \left(\frac{\partial \mu}{\partial F_Y}\right)^2 u^2(F_Y) + \left(\frac{\partial \mu}{\partial \alpha}\right)^2 u^2(\alpha) + \left(\frac{\partial \mu}{\partial \beta}\right)^2 u^2(\beta) \quad (1)$$

The partial derivatives of the friction coefficient with respect to the input variable appearing in Eq. 1 are given by Eqs. 2–5.

$$\frac{\partial \mu}{\partial F_X} = \frac{\cos\beta}{F_Y \cos\alpha + F_X \sin\beta} - \frac{\sin\beta(F_X \cos\beta - F_Y \sin\alpha)}{(F_Y \cos\alpha + F_X \sin\beta)^2} \quad (2)$$

$$\frac{\partial \mu}{\partial F_Y} = \frac{-\sin\alpha}{F_Y \cos\alpha + F_X \sin\beta} - \frac{\cos\alpha(F_X \cos\beta - F_Y \sin\alpha)}{(F_Y \cos\alpha + F_X \sin\beta)^2} \quad (3)$$

$$\frac{\partial \mu}{\partial \alpha} = \frac{-F_Y \cos\alpha}{F_Y \cos\alpha + F_X \sin\beta} + \frac{F_Y \sin\alpha(F_X \cos\beta - F_Y \sin\alpha)}{(F_Y \cos\alpha + F_X \sin\beta)^2} \quad (4)$$

Table 1 Nominal input parameters and corresponding standard uncertainties used for calculating the combined standard uncertainty of the coefficient of friction (from Eqs. 1–5) ($u_c(\mu)$)

Input	Nominal value	Standard uncertainty, u_i
Friction force (F_X)	1.26 N	10 mN
Normal load (F_Y)	6.9 N	17 μN
Angular misalignment ($\alpha = \beta$)	0.014°	0.002°
Combined standard uncertainty ($u_c(\mu)$)	0.003	

$$\frac{\partial \mu}{\partial \beta} = \frac{-F_X \sin\beta}{F_Y \cos\alpha + F_X \sin\beta} - \frac{F_X \cos\beta (F_X \cos\beta - F_Y \sin\alpha)}{(F_Y \cos\alpha + F_X \sin\beta)^2} \quad (5)$$

In this work, it has been assumed that the force axes were perpendicular (i.e., $\alpha = \beta$), which implies that $u(\alpha) = u(\beta)$, and that the load cell was aligned with the actuation axis. The partial derivatives (Eqs. 2–5) have to be evaluated at the nominal values of the input quantities.

In the present case, the nominal friction force F_X was calculated considering the average coefficient of friction measured during tribological tests performed at 6.9 N normal load (F_Y) in the presence of PAO at 423 K ($\mu = 0.18$, results presented in the following section). Table 1 reports a summary of the nominal input parameters together with their uncertainties. The uncertainty of the friction force (10 mN) was determined by calibrating the load cell with dead weights. As for the applied load, the uncertainty (17 μN) reported in Table 1 was derived from the accuracy of the scale used for measuring the dead weights. In the case of the tribological experiments presented in the manuscript, the planarity of the ATR crystal was found to be 12 ± 2 μm, which corresponds to an angular misalignment of 0.014 ± 0.002°.

The combined standard uncertainty for the coefficient of friction ($u_c(\mu)$) was then calculated using Eq. 1 and found to be 0.003. Assuming the distribution to be normal, the corresponding uncertainty accounting for 99% of the sample population, defined as three times the standard deviation, was 4% of the nominal value ($\mu = 0.18$).

4 Application: Surface-Analytical Study of Iron/Poly-α-Olefin Interactions by Means of In Situ ATR/FT-IR Tribometry

To show the usefulness of the newly developed tribological test system, ATR tribological experiments have been performed in the presence of synthetic oil (PAO) at high temperature (423 K) on iron-coated germanium ATR crystals. In the following, the experimental details and results of the tribological tests are outlined.

4.1 Experimental

4.1.1 Materials

Commercial poly-α-olefin (PAO, Durasyn® 166, Tunap Industrie GmbH & Co., Mississauga, Canada) was used as a base oil.

Trapezoidal ATR crystals of monocrystalline germanium (Graseby Specac, Portmann Instruments AG, Biel-Benken, Switzerland) with an angle of incidence of 45°, dimensions 72 × 10 × 6 mm (number of reflections, calculated according to [29], equal to 12) were used for acquiring ATR/FT-IR spectra.

In this study, the germanium ATR crystals were coated with iron by means of magnetron sputtering carried out at the Paul Scherrer Institut (Villigen, Switzerland). The planar magnetron sputtering target (ISO 9001 certified, target type PK 75) had a purity higher than 99.9%. The argon pressure during the sputtering process was 0.24 Pa and the sputtering rate was found to be 10 Å/min. The characterization by XPS of the "as received" iron-coated Ge ATR crystal is reported in [35].

In order to remove the iron coating after each experiment, the germanium ATR crystals were cleaned in a 6 M HCl solution (HCl fuming 37%, puriss p.a., Fluka, Buchs, Switzerland) first with a soaked tissue paper and afterwards by immersion in the HCl solution for at least 20 min. The crystals were then flushed with ultra-pure (Milli-Q, electrical conductivity: 18.2 MΩ cm) water and ethanol (puriss p.a., Fluka, Buchs, Switzerland) prior to being dried under a nitrogen (N5) stream. Before depositing a new iron coating on the germanium ATR crystal, a contamination check was performed by XPS.

The moving part of the tribopair, a fixed cylinder (diameter: 16 mm; width: 5.4 mm) made of stainless steel (18Cr10Ni steel), was finely machined (root-mean-square roughness (R_q, defined according to ISO 4287:1997) of the as-received cylinder: 682 ± 147 nm).

4.1.2 Methods

4.1.2.1 In Situ Attenuated Total Reflection (ATR/FT-IR) Tribometer In this study, a load cell with a maximum capacity of 5 N was mounted on the ATR/FT-IR tribometer for measuring the friction force. According to the manufacturer, the resolution of the load cell is 0.03% of the maximum capacity (i.e., 1.5 mN). The calibration of the load cell was carried out before each experiment using standard weights.

4.1.2.2 Tribological Testing In order to further reduce the surface roughness of the steel cylinder and to ensure a line contact between the cylinder and the crystal surface, the cylinders were pre-conditioned using the ATR/FT-IR

tribometer and sweeping them back and forth along a 18Cr10Ni steel bar (having the same dimensions of the ATR crystal and mounted in an ATR crystal holder), on top of which either emery paper (P1200 and P2400) or polishing cloths were fixed. After the last polishing step, performed using a 3 μm diamond paste, the cylinder was ultrasonically cleaned in ethanol (puriss p.a., Fluka, Buchs, Switzerland). Such a preparation procedure resulted in the presence of a small worn area at the bottom of the cylinder, whose width was 23 ± 3 μm. The root-mean-square roughness (R_q, defined according to ISO 4287:1997) of the as-received cylinder was 682 ± 147 nm, while that of the worn area produced on the cylinder following grinding and polishing was 187 ± 51 nm.

The tribological tests were carried out by pouring ca. 1.5 cm^3 of oil solution onto the iron-coated germanium ATR crystal and then heating the assembly to the desired temperature, i.e., 423 K. Once the desired temperature was reached (in ca. 40 min), the tribological experiment was started. In the present work, a normal load of 6.9 N (corresponding to an average contact pressure of 57 ± 10 MPa), a sliding speed of 0.5 mm/s and a stroke of 45 mm were used. During the experiments the solution was open to air. The relative humidity (RH) was measured and found to be between 22 and 33%.

ATR/FT-IR spectra were collected at 298–303 K both before and during tribological testing. Cooling the system to 298–303 K after stopping the tribotest and before the acquisition of ATR/FT-IR spectra was necessary due to the strong reduction in the transmittance of the germanium ATR element at elevated temperatures. As pointed out by Piras [17, 22], germanium becomes opaque at wavenumbers below 1600 cm^{-1} at 423 K. This effect is even more pronounced when the crystal is coated with iron: the transmittance of the iron-coated germanium crystal is almost zero over the whole spectral range at 423 K.

4.1.2.3 Fourier-Transform Infrared Spectroscopy (FT-IR) ATR/FT-IR spectra were acquired with a Nicolet™ 5700 Fourier Transform Infrared spectrometer (Thermo Electron Corporation, Madison, WI, USA) equipped with a Graseby-Specac advanced overhead (specaflow) ATR system P/N 1401 series. The experimental conditions are listed in Table 2. The diameter of the infrared beam at the entrance of the Ge ATR crystal was 4.5 mm, which made necessary the use of a cylinder (width: 5.4 mm) as a counter-surface in the tribological experiments.

4.1.3 Data Processing

The spectra were processed with OMNIC™ software (V7.2, Thermo Electron Corporation, Madison, WI, USA).

A background correction was always applied to the experimental ATR/FT-IR spectra using the single-beam spectrum of the iron-coated germanium ATR crystal collected before each experiment. The ATR/FT-IR spectra presented here are reported without any baseline and ATR correction.

Table 2 Experimental conditions for acquiring ATR/FT-IR spectra

	ATR/FT-IR
Detector	MCT/A
Beamsplitter	KBr
Spectral range (cm^{-1})	4000–600
Resolution (cm^{-1})	4
Number of scans	1024
Scan velocity (cm/s)	2.5317
Acquisition time (s)	568
Gain control	1

4.1.3.1 Variable Angle Spectroscopic Ellipsometry (VASE) The thickness of the "as-received" iron coating on the germanium ATR crystal was measured before each tribological experiment using a variable angle spectroscopic ellipsometer (VASE, M-2000 FTM, L.O.T. Oriel GmbH, Germany). Measurements were performed under ambient conditions at three different incidence angles (65°, 70° and 75°) in a spectral range of 400–700 nm. Before the analysis, the iron-coated germanium ATR crystal was flushed with ethanol (puriss p.a., Fluka, Buchs, Switzerland) and dried under a nitrogen (N5) stream. Spectroscopic scans were taken every 5 mm along the sample for a total of 10 spots. The beam diameter is estimated to be below 1 mm.

Data processing was performed using WVASE32® software (J.A. Wollman Co., Inc., Lincoln, NE, USA) applying a multilayer model, which consisted of a germanium substrate (assumed to be semi-infinite), a metallic iron layer and an iron oxide (hematite, α-Fe_2O_3) layer. While the optical constants (refractive index n, extinction coefficient k) of germanium, metallic iron and iron oxide were kept fixed during data evaluation, the thickness of the metallic iron and iron oxide layers were determined by fitting $\Psi(\lambda)$ and $\Delta(\lambda)$. The optical constants of the three layers as a function of the wavelength are reported in [35].

The thickness values of the metallic iron (10.7 ± 0.1 nm) and iron oxide (1.7 ± 0.1 nm) layers of the samples used in this work are the same of those reported in [35].

4.1.3.2 Profilometry A Sensofar PLu Neox (Sensofar-Tech, SL., Terrassa, Spain) 3D optical profiler was used for characterizing the ATR crystal surface at the end of the tribological tests. Data acquisition and data processing were carried out with SensoSCAN® software (v.3.1.1.1, Sensofar-Tech, SL., Terrassa, Spain) and SensoMAP software (v.5.1.1., Digital Surf, Besancon, France), respectively.

All the measurements were performed using the confocal method with a 50× objective (vertical resolution <1 nm [36]).

The roughness of the as-received (i.e., not-coated) and iron-coated germanium ATR crystal was also measured by profilometry (white-light interferometry) and found to be 1.5 ± 0.1 nm and 1.3 ± 0.1 nm, respectively.

4.2 Results

4.2.1 Tribological Testing

Figure 4 displays an example of the evolution of the coefficient of friction (CoF) during a tribological test performed in the presence of pure PAO at 423 K. The CoF was found to decrease with the sliding time and to level off at ~0.15 after 300 cycles.

The standard deviation of the CoF, calculated considering the data points corresponding to a cylinder position between 1/6 and 5/6 of the stroke length, is also plotted as a function of the number of cycles (sliding time) in Fig. 4 (top part). While the standard deviation is constant in the first part of the tribotest, it showed an irregular behavior in the last 150 cycles.

4.2.2 Attenuated Total Reflection (ATR/FT-IR) Spectroscopy

The ATR/FT-IR spectra acquired during tribological testing on an iron-coated (10 nm) germanium ATR crystal in the presence of pure PAO at 423 K are reported in Fig. 5.

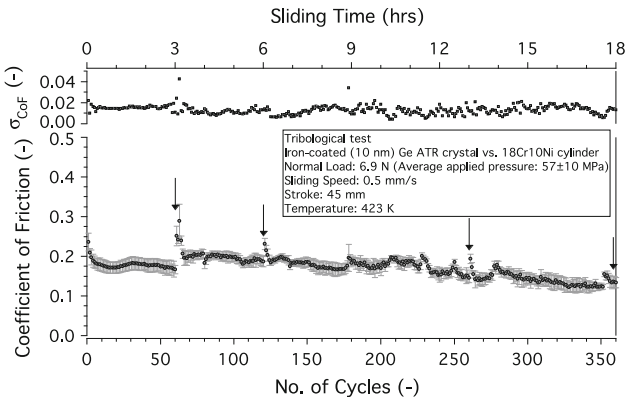

Fig. 4 Coefficient of friction (CoF) versus number of cycles (sliding time) during tribological tests (normal load: 6.9 N; sliding speed: 0.5 mm/s, stroke: 45 mm) performed in the presence of pure PAO at 423 K. In order to calculate the average CoF and the corresponding standard deviation over one sliding cycle, only the data points corresponding to a cylinder position between 1/6 and 5/6 of the stroke length were considered. The standard deviation is plotted as a function of the number of cycles (sliding time) in the *top part of the graph*. The ATR/FT-IR spectra were acquired periodically during the tribotests (*arrows*)

The spectrum collected before starting sliding (0 h) showed the characteristic IR absorption bands of PAO at 2952 cm^{-1} ($\nu_{as}CH_3$), 2917 cm^{-1} ($\nu_{as}CH_2$), 2870 cm^{-1} (ν_sCH_3), 2849 cm^{-1} (ν_sCH_2), 1454 cm^{-1} ($\delta_{as}CH_3$, δCH_2) and 1376 cm^{-1} (δ_sCH_3) [37–39].

Upon tribotesting at 423 K for 3 h, weak signals were detected in the fingerprint region and could be assigned to the characteristic vibrations of carboxylate salts and carbonate complexes (monodentate and bidentate) [37, 39–44]: in the 1600–1500 cm^{-1} region, where the $\nu_{as}CO_2^-$ vibration of carboxylate salts as well as the $\nu_{as}CO_2^-$ and ν_{as}C-O vibrations of, respectively, monodentate and bidentate carbonate complexes are found, two peaks appeared at 1558 and 1511 cm^{-1}, whereas a weak band at 1251 cm^{-1} was detected and assigned to the $\nu_{as}CO_2^-$ (bidentate) vibration in carbonate complexes. The spectrum also showed the appearance of an absorption band at 877 cm^{-1}, which corresponds to the bending vibration of the carbonate anion (δC–O). Moreover, after 6 h a new weak and broad peak, which became more intense after 12 and 18 h, was detected in the 1850-1550 cm^{-1} region (with maxima at 1711 and 1722 cm^{-1}), where the C=O stretching vibration (νC=O) occurs. The IR peaks and the assigned functional groups are listed in Table 3.

Upon tribotesting at 423 K, a progressive variation of the baseline of the ATR/FT-IR spectra was observed.

4.2.3 Profilometry

At the end of the tribological tests performed at 423 K for 18 h in the presence of pure PAO, the ATR crystal surface was characterized by optical profilometry.

The wear tracks generated on the iron-coated (10 nm) germanium ATR crystal showed the presence of several and distinct scars, which were evenly distributed in the tribostressed region and parallel to the sliding direction (Fig. 6a). The 2D surface topography of a tribostressed iron-coated germanium ATR crystal is depicted in Fig. 6b, whereas Fig. 6c displays the extracted profiles. Grooves as deep as 2 μm were found on the iron-coated (10 nm) germanium ATR crystal.

4.3 Discussion

4.3.1 Comparison of the Newly Developed In Situ Tribological System with Other In Situ Approaches in Tribology

A tribological test system, based on ATR/FT-IR spectroscopy [17–19, 22], for the in situ characterization of boundary lubricant layers formed by oil additives, has been improved by the incorporation of a force-measuring system. This allowed the measurement of the friction force

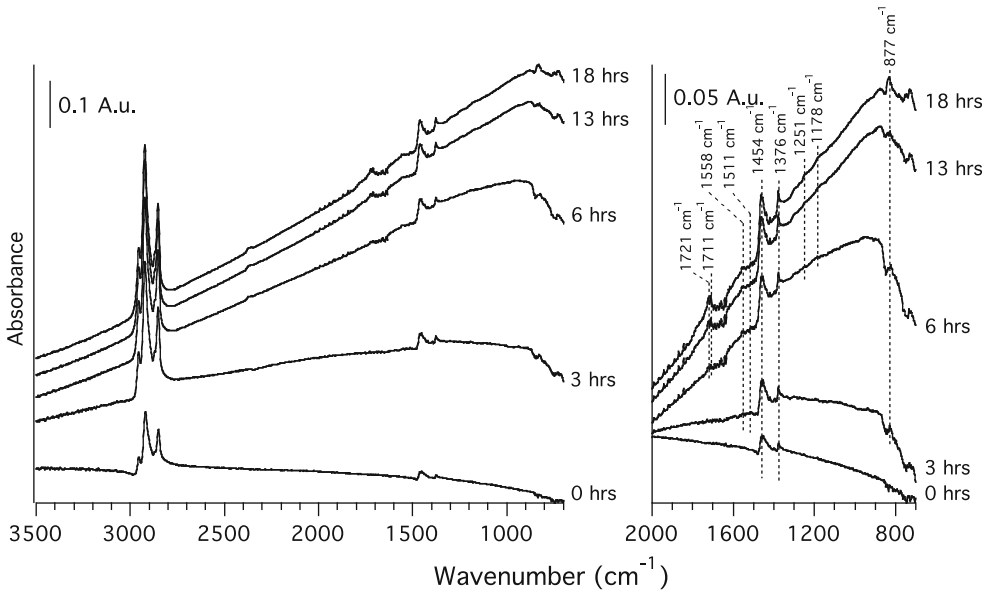

Fig. 5 ATR/FT-IR spectra collected during a tribological test performed in the presence of pure PAO at 423 K on an iron-coated (10 nm) Ge ATR crystal. *Left* whole spectral region. *Right* fingerprint region

Table 3 IR frequencies (cm^{-1}) and functional groups for the ATR/FT-IR spectra acquired during tribological testing at 423 K in the presence of Pure PAO on iron-coated (10 nm) Ge ATR crystal

Frequency (cm^{-1})	Functional Group
2952, 2917, 2870, 2849	$\nu_{as}CH_3$, $\nu_{as}CH_2$, ν_sCH_3, ν_sCH_2
1721, 1711	νC=O
1558, 1511	$\nu_{as}CO_2^-$ (carboxylate salts and carbonate complexes), ν_{as}C–O (carbonate complexes)
1454	$\delta_{as}CH_3$, δCH_2
1376	δ_sCH_3
1251	$\nu_{as}CO_2^-$ (carbonate complexes)
877	δC-O

Counter-surface: 18Cr10Ni cylinder

ν stretching, δ in-plane deformation vibration

during tribological experiments and its correlation with the chemical reactions taking place at the metal/oil interface.

Several of the in situ approaches for tribological studies proposed in the last decade are based on ultra-high vacuum (UHV) surface-analytical techniques, such as XPS [45–47], PEEM [48], AES [45–47, 49], and TEM [50]. The ultra-high vacuum (UHV) environment inhibits their use for the investigation of oil-lubricated tribological systems. Recently, the introduction of specific gases with the same chemical functionality of the additive under investigation inside the UHV chamber has been proposed as an effective method for reproducing, simplifying and better understanding complex tribochemical mechanisms [51, 52]. However, the absence of any base oil, which might become oxidized during the tests unless it is blended with additives having antioxidant properties, can strongly affect the surface-reaction mechanism of the additive under investigation, and therefore makes this approach not an ideal simulation of real lubricated systems.

Vibrational spectroscopies, not requiring ultra-high vacuum for carrying out analytical studies, provide valuable insights into the chemical reactions taking place within the rubbing interface [4–22]. Although the literature demonstrated the possibility of investigating the chemical composition [23–25] and the conformation of the lubricant film [15, 26], the pressure distribution within the contact [27] as well as the third bodies formed by solid lubricants in the contact [4–12], the necessity of replacing one of surfaces with an IR-transparent window can have significant implications for the study of the tribochemistry of lubricant additives and solid lubricants. Such a requirement was found not to strongly affect the studies of fluid lubricating film behavior performed by infrared micro-reflection spectroscopy: the tribotests, in this case, were carried out in the elasto-hydrodynamic (EHL) regime and, therefore, infrared spectroscopy was not used as a surface-sensitive technique [15, 23–27].

Conversely, in the case of the in situ Raman tribometer developed by Singer et al. for the investigation of the influence of the morphology, structure, chemistry and motion of third bodies on the friction and wear of solid lubricants [4–12], one of the sliding surfaces had to be transparent to the wavelength of radiation concerned. Although this in situ tribological test system allowed the correlation of the Raman results with the frictional changes/instabilities and, therefore, allowed conclusions to be drawn concerning the velocity-accommodation mechanism of solid lubricants, the underlying tribological mechanism leading to the formation of third bodies might be different in the case of self-mated surfaces.

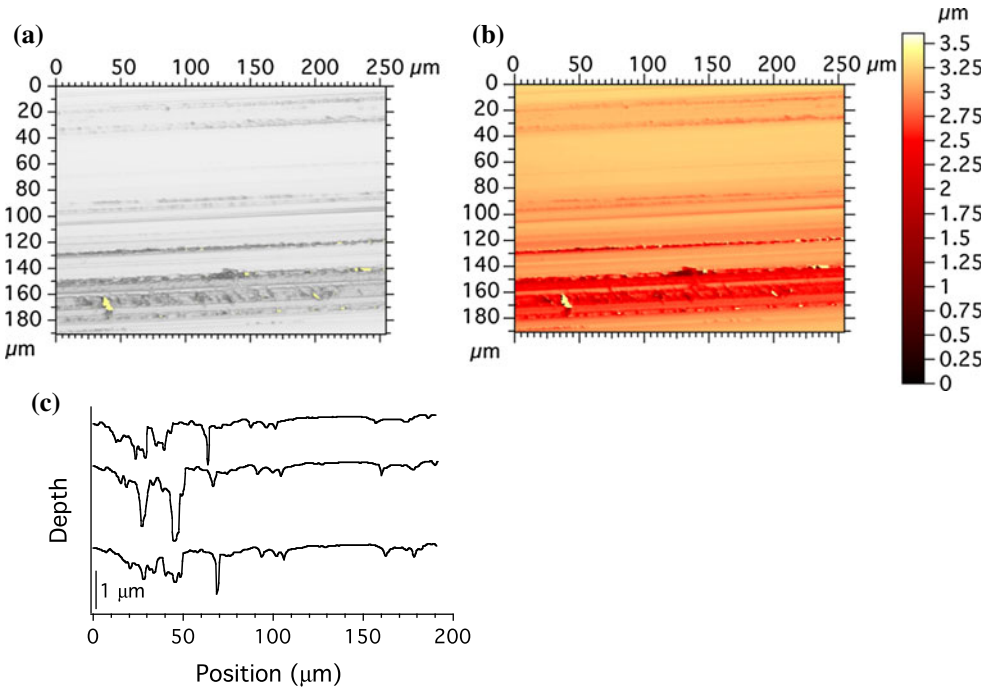

Fig. 6 Bright-field image (**a**) and 2D surface topography (**b**) of an iron-coated (10 nm) Ge ATR crystal tribostressed at 423 K for 18 h in the presence of pure PAO. The profiles extracted (perpendicular to the sliding direction) from **b** are reported in **c**

The in situ ATR/FT-IR tribological test system presented in this work combines the possibility of measuring the friction force during the tribological test with the analysis of the sample through a thin metal film representing one surface of the tribopair. In this way, technological systems are effectively modeled from both a contact mechanical (i.e., applied load and sliding speed) and surface chemical (iron vs. steel) point of view. The necessity of stopping the tribological test and lifting the counter-surface (i.e., the cylinder) over the ATR crystal during the acquisition of the ATR/FT-IR spectra classifies this approach as in situ-*post mortem* [1], however.

4.3.2 *Correlation of the Friction Results with the ATR/FT-IR Spectra Acquired During Tribotests Performed in the Presence of Pure PAO*

The ATR/FT-IR spectra acquired during tribological testing at 423 K in the presence of pure PAO using a fixed 18Cr10Ni steel cylinder sliding on an iron-coated (10 nm) ATR germanium crystal indicated the occurrence of a surface reaction on the air-oxidized iron-coated Ge ATR crystal surface to give carbonate complexes and carboxylate salts (Table 3).

The formation of iron complexes upon tribotesting in the presence of hydrocarbons at elevated temperatures on iron surfaces has already been reported in the literature [35, 53–58]. Cadvar and Ludema, who studied the tribochemistry of additive-free mineral oils on steel surfaces at room temperature with a step loading of 62.5 N up to a maximum applied load of 1890 N, showed by in situ ellipsometry the formation of a 5–10 nm thick layer consisting of organic compounds with iron on top of the oxide/carbide substrate [53]. On the other hand, the analysis by gel-permeation chromatography of oil samples used to lubricate sliding contacts, showing the presence of organo-iron species with molecular weights up to 100,000 in the lubricants, led Hsu to hypothesize that the metal-catalyzed oil oxidation leads to the formation of polymers through condensation reactions on top of the metal surface [54, 55].

The ATR/FT-IR results outlined in this study could be explained considering the chemical species produced during the thermal degradation of the base oil. As already demonstrated in our previous works [59, 60] and as extensively reported in the literature [61], hydrocarbons, such as PAO, are susceptible to thermo-oxidative aging, which leads to the production of oxygenated compounds, such as carboxylic acids. The detection of an absorption band, which could be assigned to the carbonyl stretching vibration, in the ATR/FT-IR spectra acquired upon sliding for more than 3 h and in the transmission FT-IR spectrum of the oil solution used for running the tribotests (analysis performed at the end of the tribological experiment. Spectrum not shown) clearly indicates the formation of oxygenated species in the bulk oil. These molecules, whose production is catalyzed by transition-metal ions having two valence states (e.g., $Fe^{2+/3+}$), can adsorb onto the metal surface and react with it, forming metal complexes [53, 54], as observed in this work.

The changes detected in the ATR/FT-IR spectra upon tribotesting at 423 K in the presence of PAO are similar to those observed in the ATR/FT-IR spectra acquired during control experiments performed under the same experimental

conditions, but without any sliding [35]. However, while in the case of the spectra acquired under purely thermal conditions the intensity of the absorption bands, which suggested the formation of a reaction layer consisting of carbonate complexes and carboxylate salts, was found to increase with the heating time [35], in the case of the tribological experiments reported in this study the absorbance of the new peaks appearing in the ATR/FT-IR spectra did not increase with the sliding time, indicating that the surface reaction products are progressively removed upon rubbing. This finding correlates with the changes in the friction force detected during the tribological tests. In particular, the irregular behavior of the CoF standard deviation upon tribotesting for more than 150 cycles corresponds to the wearing of the iron-coated germanium ATR crystal. The optical profilometry results, which indicated the presence of grooves as deep as 2 μm generated on the iron-coated (10 nm) germanium ATR crystal by sliding a fixed cylinder made of stainless steel, further support the wearing of the substrate, i.e., the iron-coated germanium ATR crystal. Note: in a sense, this experiment represents the harshest conditions for such a setup, since the majority of experiments would be testing lubricants containing anti-wear additives!

4.3.3 Comparison of the Extended ATR/FT-IR Tribometer with a Commercially Available Tribometer

Tribological measurements with the extended ATR/FT-IR tribometer developed in the present work were compared with a commercially available tribometer, namely the CETR UMT-2 tribometer (Center for Tribology, Campbell CA, USA). The latter significantly differs from the ATR/FT-IR tribological test system: it incorporates a two-dimensional load cell and the samples are fixed on stages having encoders to monitor their position and moving direction. The extended ATR/FT-IR tribometer, on the other hand, uses a one-dimensional load cell and does not have any encoder. More details about the CETR UMT-2 tribometer can be found in [62, 63].

In order to compare the tribological results obtained with the two systems, comparison tests were carried out in pure PAO, at room temperature and using a 18Cr10Ni steel cylinder sliding on a 18Cr10Ni steel bar (cylinder-on-flat configuration, reciprocating motion). The 18Cr10Ni steel bars were mechanically polished with a 1/4 μm diamond paste. The 18Cr10Ni steel cylinders were prepared following the procedure reported in Sect. 4.1.2.2.

Figure 7 displays the coefficient of friction values measured during tribological tests performed at two different loads, i.e., 900 and 2900 mN, using the CETR UMT-2 and ATR/FT-IR tribometer under the same experimental conditions. The friction results obtained with the two test systems were comparable at both applied loads.

5 Conclusions

A new in situ tribometer, based on attenuated total reflection Fourier-transform infrared (ATR/FT-IR) spectroscopy, has been developed for investigating tribochemistry at the lubricant–substrate interface. The incorporation of a force-measuring system allowed the measurement of the friction force during tribological experiments and its correlation

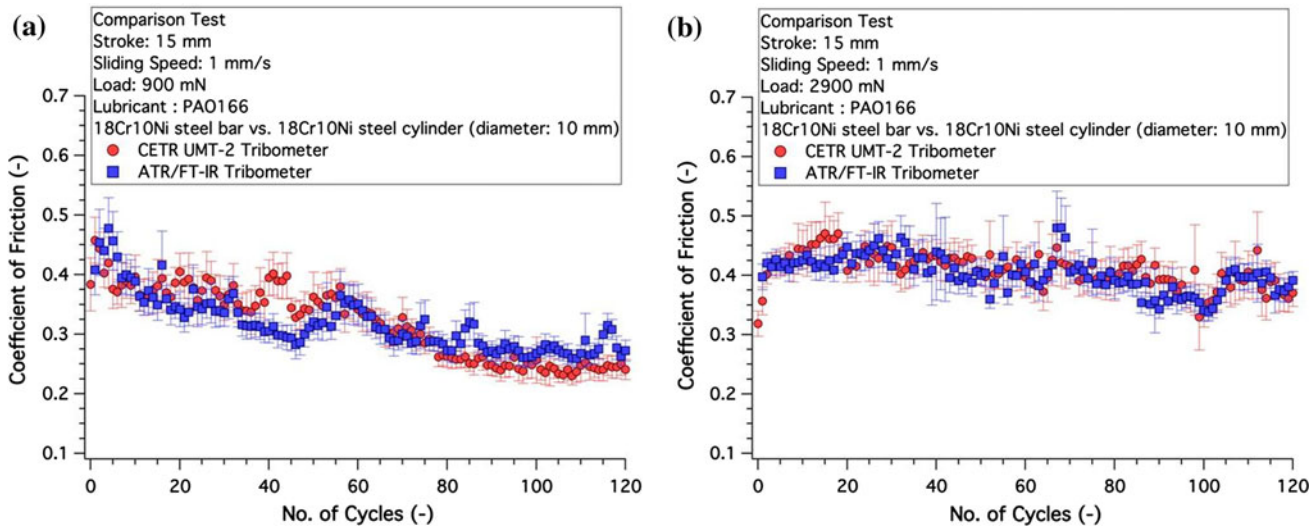

Fig. 7 Coefficient of friction (CoF) versus number of cycles during tribological tests performed at 900 mN (**a**) and 2900 mN (**b**) in pure PAO, at room temperature and using a 18Cr10Ni steel cylinder sliding on a 18Cr10Ni steel bar (cylinder-on-flat configuration, reciprocating motion). The stroke was 15 mm and the sliding speed was 1 mm/s. The *error bars* show the standard deviation of the CoF during one cycle (considering the data points corresponding to a slider position between 1/6 and 5/6 of the stroke length)

with infrared spectroscopic results that provide insights into the chemical reactions taking place at the metal/oil interface. The usefulness of the newly developed tribological test system has been demonstrated by performing ATR/FT-IR tribotests in the presence of synthetic oil (PAO) at high temperature (423 K) on iron-coated germanium ATR crystals. An uncertainty analysis was carried out for the new in situ tribometer and revealed the possibility of measuring coefficients of friction with an accuracy of 0.003 under the experimental conditions employed for performing the tribological tests reported in the work.

Acknowledgments The authors wish to express their gratitude to the ETH Research Commission for its support of this work. Mr. M. Horisberger kindly prepared the iron coatings by magnetron sputtering at PSI (Villigen, Switzerland). Finally, the authors would like to gratefully acknowledge Mr. M. Elsener for the mechanical modifications of the ATR/FT-IR tribometer.

References

1. Donnet, C.: Problem-solving methods in tribology with surface-specific techniques. In: Rivière, J.C., Myhra, S. (eds.) Handbook of Surface and Interface Analysis: Methods and Problem-Solving. Marcel Dekker Inc., New York (1998)
2. Gellman, A.J., Spencer, N.D.: Surface chemistry in tribology. J. Eng. Tribol. **216**(6), 443–461 (2002)
3. Sawyer, W.G., Wahl, K.J.: Accessing Inaccessible Interfaces: in situ approaches to materials tribology. MRS Bull. **33**, 1145–1150 (2008)
4. Chromik, R.R., Baker, C.C., Voevodin, A.A., Wahl, K.J.: In situ tribometry of solid lubricant nanocomposite coatings. Wear **262**(9–10), 1239–1252 (2007)
5. Chromik, R.R., Winfrey, A.L., Lüning, J., Nemanich, R.J., Wahl, K.J.: Run-in behavior of nanocrystalline diamond coatings studied by in situ tribometry. Wear **265**(3–4), 477–489 (2008)
6. Dvorak, S., Wahl, K.J., Singer, I.L.: In situ analysis of third body contributions to sliding friction of a Pb–Mo–S coating in dry and humid air. Tribol. Lett. **28**(3), 263–274 (2007)
7. Dvorak, S.D., Wahl, K.J., Singer, I.L.: Friction behavior of boric acid and annealed boron carbide coatings studied by in situ Raman tribometry. Tribol. Trans. **45**(3), 354–362 (2002)
8. Scharf, T.W., Singer, I.L.: Role of third bodies in friction behavior of diamond-like nanocomposite coatings studied by in situ tribometry. Tribol. Trans. **45**(3), 363–371 (2002)
9. Scharf, T.W., Singer, I.L.: Monitoring transfer films and friction instabilities with in situ Raman tribometry. Tribol. Lett. **14**(1), 3–8 (2003)
10. Scharf, T.W., Singer, I.L.: Quantification of the thickness of carbon transfer films using Raman tribometry. Tribol. Lett. **14**(2), 137–145 (2003)
11. Singer, I.L., Dvorak, S.D., Wahl, K.J., Scharf, T.W.: Role of third bodies in friction and wear of protective coatings. J. Vac. Sci. Technol. **21**(5), S232–S240 (2003)
12. Wahl, K.J., Chromik, R.R., Lee, G.Y.: Quantitative in situ measurement of transfer film thickness by a Newton's rings method. Wear **264**(7–8), 731–736 (2008)
13. Wahl, K.J., Sawyer, W.G.: Observing interfacial sliding processes in solid–solid contacts. MRS Bull. **33**, 1159–1167 (2008)
14. Cann, P.M.: In-contact molecular spectroscopy of liquid lubricant films. MRS Bull. **33**, 1151–1158 (2008)
15. Cann, P.M., Spikes, H.A.: In-contact IR spectroscopy of hydrocarbon lubricants. Tribol. Lett. **19**(4), 289–297 (2005)
16. Olsen, J.E., Fischer, T.E., Gallois, B.: In situ analysis of the tribochemical reactions of diamond-like carbon by internal reflection spectroscopy. Wear **200**(1–2), 233–237 (1996)
17. Piras, F.M., Rossi, A., Spencer, N.D.: Growth of tribological films: in situ characterization based on attenuated total reflection infrared spectroscopy. Langmuir **18**(17), 6606–6613 (2002)
18. Piras, F.M., Rossi, A., Spencer, N.D.: In situ attenuated total reflection (ATR) spectroscopic analysis of tribological phenomena. Boundary and mixed lubrication: science and applications. In: Proceedings of the 28th Leeds-Lyon Symposium. Elsevier Science B.V., Lyon, 2002
19. Piras, F.M., Rossi, A., Spencer, N.D.: Combined in situ (ATR FT-IR) and ex situ (XPS) study of the ZnDTP-iron surface interaction. Tribol. Lett. **15**(3), 181–191 (2003)
20. Rossi, A., Piras, F.M., Kim, D., Gellman, A.J., Spencer, N.D.: Surface reactivity of tributyl thiophosphate: effects of temperature and mechanical stress. Tribol. Lett. **23**(3), 197–208 (2006)
21. Sasaki, K., Inayoshi, N., Tashiro, K.: Development of new in situ observation system for dynamic study of lubricant molecules on metal friction surfaces by two-dimensional fast-imaging Fourier-transform infrared-attenuated total reflection spectrometer. Rev. Sci. Instrum. **79**(12), 123702–123707 (2008)
22. Piras, F.M.: In Situ Attenuated Total Reflection Tribometry. PhD Thesis no. 14638. ETH Zurich, Zurich, Switzerland (2002)
23. Cann, P.M., Spikes, H.A.: Fourier-transform infrared study of the behavior of grease in lubricated contacts. Lubr. Eng. **48**, 335–343 (1992)
24. Hurley, S., Cann, P.M.: IR spectroscopic analysis of grease lubricant films in rolling contacts. In: 25th Leeds-Lyon Symposium On Tribology, pp. 589–600, 1999
25. Hurley, S., Cann, P.M., Spikes, H.A.: Lubrication and reflow properties of thermally aged greases. Tribol. Trans. **43**(1), 9–14 (2000)
26. Beattie, D., Winget, S., Bain, C.: Raman scattering from confined liquid films in the sub-nanometre regime. Tribol. Lett. **27**(2), 159–167 (2007)
27. Jubault, I., Mansot, J.L., Vergne, P., Mazuyer, D.: In situ pressure measurements using Raman microspectroscopy in a rolling elastohydrodynamic contact. J. Tribol. **124**(1), 114–120 (2002)
28. Bürgi, T., Baiker, A.: Attenuated total reflection infrared spectroscopy of solid catalysts functioning in the presence of liquid-phase reactants. In: Bruce, C.G., Helmut, K. (eds.) Advances in Catalysis, pp. 227–283. Academic Press, San Diego (2006)
29. Harrick, N.J.: Internal Reflection Spectroscopy, p. 327. Interscience Publishers, New York (1967)
30. ASTM International G 133-05: Standard Test Method for Linearly Reciprocating Ball-on-Flat Sliding Wear. ASTM International, Washington (2005)
31. Burris, D., Sawyer, G.W.: Addressing practical challenges of low friction coefficient measurements. Tribol. Lett. **35**(1), 17–23 (2009)
32. Schmitz, T.L., Action, J.E., Ziegert, J.C., Sawyer, G.W.: The difficulty of measuring low friction: uncertainty analysis for friction coefficient measurements. J. Tribol. **127**(3), 673–678 (2005)
33. Fornasini, P.: The Uncertainty in Physical Measurements. An Introduction to Data Analysis in the Physics Laboratory. Springer, New York (2008)
34. Taylor, J.R.: An Introduction to Error Analysis: The Study of Uncertainties in Physical Measurements. University Science Book, Sausalito (1997)
35. Mangolini, F., Rossi, A., Spencer, N.D.: Chemical reactivity of triphenyl phosphorothionate (TPPT) with iron: an ATR/FT-IR

and XPS investigation. J. Phys. Chem. C **115**(4), 1339–1354 (2010)
36. Sensofar-Tech: PLu Neox 3D Optical Profiler. Sensofar-Tech, Terrassa (2009)
37. Colthup, N.B., Daly, L.H., Wiberley, S.E.: Introduction to Infrared and Raman Spectroscopy, 3rd edn. Academic Press, London (1990)
38. Roeges, N.P.G.: A Guide to the Complete Interpretation of Infrared Spectra of Organic Structures. Wiley, Chichester (1994)
39. Socrates, G.: Infrared and Raman Characteristic Group Frequencies, 3rd edn. Wiley, Chichester (2001)
40. Nakamoto, K.: Infrared and Raman Spectra of Inorganic and Coordination Compounds. Part A: Theory and Applications in Inorganic Chemistry, 5th edn. Wiley, New York (1997)
41. Bargar, J.R., Kubicki, J.D., Reitmeyer, R., Davis, J.A.: ATR-FTIR spectroscopic characterization of coexisting carbonate surface complexes on hematite. Geochim. Cosmochim. Acta **69**(6), 1527–1542 (2005)
42. Rèmazeilles, C., Refait, P.: Fe(II) hydroxycarbonate $Fe_2(OH)_2CO_3$ (chukanovite) as iron corrosion product: synthesis and study by Fourier transform infrared spectroscopy. Polyhedron **28**(4), 749–756 (2009)
43. Roonasi, P., Holmgren, A.: An ATR-FTIR study of carbonate sorption onto magnetite. Surf. Interface Anal. **42**(6–7), 1118–1121 (2010)
44. Wijnja, H., Schulthess, C.P.: Carbonate adsorption mechanism on goethite studied with ATR-FTIR, DRIFT, and proton coadsorption measurements. Soil Sci. Soc. Am. J. **65**(2), 324–330 (2001)
45. Boehm, M., Martin, J.-M., Grosslord, C., Le Mogne, Th.: Modelling tribochemical reactions of additives by gas-phase lubrication. Tribol. Lett. **11**(2), 83–90 (2001)
46. Martin, J.-M., Liang, H., Le Mogne, Th., Malroux, M.: Low-temperature friction in the XPS analytical ultrahigh vacuum tribotester. Tribol. Lett. **14**(1), 25–31 (2003)
47. Martin, J.-M., Le Mogne, Th., Boehm, M., Grosslord, C.: Tribochemistry in the analytical UHV tribometer. Tribology International **32**(11), 617–626 (1999)
48. Montei, E.L., Kordesch, M.E.: Detection of tribochemical reactions using photoelectron emission microscopy. In: The 42nd national symposium of the American Vacuum Society. AVS, Mineapolis, 1996
49. Glaeser, W.A., Baer, D., Engelhardt, M.: In situ wear experiments in the scanning Auger spectrometer. Wear **162–164**(Part 1), 132–138 (1993)
50. Marks, L.D., Warren, O.L., Minor, A.M., Merkle, A.P.: Tribology in full view. MRS Bull. **33**, 1169–1173 (2008)
51. Philippon, D., De Barros-Bouchet, M.I., Le Mogne, Th., Lerasle, O., Bouffet, A., Martin, J.-M.: Role of nascent metallic surfaces on the tribochemistry of phosphite lubricant additives. Tribol. Int. **44**(6), 684–691 (2010)
52. Philippon, D., De Barros-Bouchet, M.I., Lerasle, O., Le Mogne, Th., Martin, J.M.: Experimental simulation of tribochemical reactions between borates esters and steel surface. Tribol. Lett. **41**, 73–82 (2011)
53. Cavdar, B., Ludema, K.C.: Dynamics of dual film formation in boundary lubrication of steels part II. Chemical analyses. Wear **148**(2), 329–346 (1991)
54. Hsu, S.M.: Boundary lubrication: current understanding. Tribol. Lett. **3**(1), 1–11 (1997)
55. Hsu, S.M., Klaus, E.E., Cheng, H.S.: A mechano-chemical descriptive model for wear under mixed lubrication conditions. Wear **128**(3), 307–323 (1988)
56. Armstrong, R.D., Hall, C.A.: The corrosion of metals in contact with ester oils containing water at 60 and 150°C. Electrochim. Acta **40**(9), 1135–1147 (1995)
57. Jayadas, N.H., Nair, K.P.: Elucidation of the corrosion mechanism of vegetable-oil-based lubricants. J. Tribol. **129**(2), 419–423 (2007)
58. Van Ooij, W.J., Rangarajan, V.: Mechanism of adhesion between polyolefins and steel as studied by XPS and static SIMS. MRS Symp. Proc. **119**, 241–246 (1988)
59. Mangolini, F., Rossi, A., Spencer, N.D.: Reactivity of triphenyl phosphorothionate in lubricant oil solution. Tribol. Lett. **35**(1), 31–43 (2009)
60. Mangolini, F., Rossi, A., Spencer, N.D.: Influence of metallic and oxidized iron/steel on the reactivity of triphenyl phosphorothionate in oil solution. Tribol. Int. **44**(6), 670–683 (2010)
61. Rasberger, M.: Oxidative degradation and stabilization of mineral oil based lubricants. In: Mortier, R.M., Orszulik, S.T. (eds.) Chemistry and Technology of Lubricants, pp. 98–143. Blackie Academic & Professional, London (1997)
62. Eglin, M.: Development of a Combinatorial Approach to Lubricant Additive Characterization. PhD Thesis no. 15054. ETH Zurich, Zurich, Switzerland
63. Heuberger, R.: Combinatorial Study of the Tribochemistry of Anti-Wear Lubricant Additives. PhD Thesis no. 17207. ETH Zurich, Zurich, Switzerland